Chapter 5

System: HF

State-selective control of molecular dynamics with ultrashort laser pulses, in particular, complete localization of population at a selected energy level on the picosecond and femtosecond time scales is a very promising line in molecular physics and has attracted much interest recently (see, for example, Refs. [14, 103, 132–137] and references therein). Until now, the ultrafast population transfer on the picosecond and femtosecond time scales has been simulated for vibrational [14, 132–137] and vibronic [103] transitions, neglecting the molecular rotational motion. Ultrafast selective preparation of the vibrational-rotational states with infrared (IR) laser pulses has not been extensively studied yet. For example, the multiphoton IR excitation and dissociation of the rotating HF molecule has been simulated in Ref. [138] by making use of chirped laser pulses, and in Ref. [121] by making use of the optimal control theory (OCT), but the state-selectivity of the process has not been studied therein.

The well-known adiabatic passage approach for the coherent population transfer between the vibrational-rotational states of diatomic molecules in the ground electronic state (see Ref. [139] and references therein) is realized on a nanosecond time scale only and makes use of the the excited electronic state as the intermediate one (the lambda-type level configuration).

In this work an alternative approach to multiphoton excitation and dissociation of rotating diatomic molecules is presented. The approach is demonstrated on the picosecond time scale and based on a reasonable choice of the excitation and dissociation pathways solely in the ground electronic state, where use is made of a constructive interference of different excitation routes and state-selective overtone transitions. Two examples of highly efficient control shall be presented: the complete, 100% population transfer between the bound vibrational-rotational states (which makes it possible to prepare a specified state selectively by making use of one or more laser pulses), and efficient, close to 100%, dissociation from selectively prepared moderately high vibrational-rotational states. Both the preparation and dissociation are controlled by optimal linearly polarized shaped picosecond IR laser pulses.

Until now, close to 100% dissociation on the picosecond time scale has been simulated only for rotationless models of diatomic molecules [14, 20, 140], where molecular dipoles are aligned along the electric field axis of a linearly polarized laser pulse. Such an approximation can not be used when dealing with rotating molecules, and basically new control schemes should be designed to control dissociation with almost 100% probability.

The results presented in this chapter have been published in [141]. The methodology of control in presence of rotation was developed by Dr. G.K. Paramonov, whereas the routine optimizations of the laser pulse parameters were performed by the author of the thesis.

5.1 Model and techniques

As a model system, the HF molecule in the ground electronic state is considered. The molecular parameters are adapted from Ref. [121]. Specifically, the potential energy curve is of the Morse form,

$$U(r) = D_e\{\exp[-2\beta_e(r-r_e)] - 2\exp[-\beta_e(r-r_e)]\}, \tag{5.1}$$

where the well depth is $D_e = 0.225009\, E_H$, the Morse parameter $\beta_e = 1.174014\, a_0^{-1}$, and the equilibrium distance is $r_e = 1.732516\, a_0$ (E_H is the Hartree energy and a_0 is the Bohr radius).

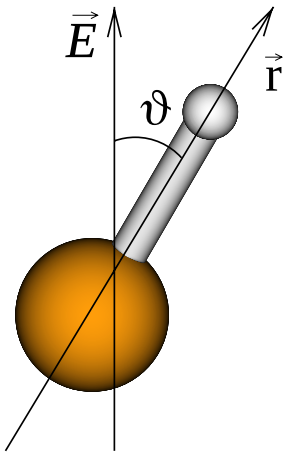

Figure 5.1: Coordinate system for the rotating HF molecule. $\hat{r}$ is the molecular axis, $\hat{E}$ is the axis of the laser electric field, and ϑ is the angle between them.

Initially, at $t = 0$, the HF molecule is assumed to be in the ground vibrational ($v = 0$) and ground rotational ($j = 0$) state, which implies that an initial temperature is less than about 10 K. Such a molecule is described by a three-dimensional Hamilton operator

$$\hat{\mathrm{H}}_{\mathrm{mol}}(r,\vartheta,\phi) = -\frac{\hbar^2}{2m_r}\frac{\partial^2}{\partial r^2} - \frac{\hbar^2}{2m_r r^2}\frac{1}{\sin\vartheta}\frac{\partial}{\partial\vartheta}\sin\vartheta\frac{\partial}{\partial\vartheta} - \frac{\hbar^2}{2m_r r^2\sin^2\vartheta}\frac{\partial^2}{\partial\phi^2} + U(r), \tag{5.2}$$

where ϕ is the asimuthal angle. Since the linearly polarized laser fields are to be used, the magnetic quantum number $m = 0$ is conserved, and the molecule is described by the azimuthally symmetric two-dimensional molecular Hamiltonian

$$\hat{\mathrm{H}}_{\mathrm{mol}}(r,\vartheta) = -\frac{\hbar^2}{2m_r}\frac{\partial^2}{\partial r^2} + U(r) - \frac{\hbar^2}{2m_r r^2}\frac{1}{\sin\vartheta}\frac{\partial}{\partial\vartheta}\sin\vartheta\frac{\partial}{\partial\vartheta} \tag{5.3}$$

where the reduced mass is $m_r = 1744.63207\, m_e$ (m_e being the electron rest mass), and ϑ is the angle between the molecular axis and the laser electric-field axis (see

Figure 5.1). Interaction with the laser field is treated semiclassically, by the interaction Hamiltonian

$$\hat{\mathrm{H}}_{\mathrm{int}}(r,\vartheta,t) = -\,\mu(r)\cos\vartheta\,\mathcal{E}(t), \tag{5.4}$$

where $\mathcal{E}(t)$ is the laser electric-field strength, and the molecular dipole moment function is $\mu(r) = \mu_0 r \exp(-\gamma\, r^4)$, with $\mu_0 = 0.454141\, e$ (e is the elementary charge), and $\gamma = 0.0064\, a_0^{-4}$.

The laser fields to be used below for state-selective vibrational-rotational excitation and dissociation of HF may be composed of several $\sin^2$-shaped pulses,

$$\mathcal{E}(t) = \sum_n \mathcal{E}_n \sin^2[\pi(t - t_{0n})/t_{pn}] \cos[\omega_n(t - t_{0n}) + \varphi_n], \tag{5.5}$$

where the nth pulse starts at $t = t_{0n}$, its duration is t_{pn}, the pulse amplitude is $\mathcal{E}_n$, and ω_n is the carrier frequency. The phases φ_n proved to be of minor importance, and the results below are presented for $\varphi_n = 0$. The $\sin^2$-shape of the laser pulses used here as in Refs. [14, 20, 103, 132, 135–137] is suitable, but rather arbitrary — similar results can be obtained by using other reasonable, "bell"-type, shapes of the pulses, for example, Gaussian.

As an absorbing boundary condition at large r use is made of the imaginary optical potential with exponential damping, similar to the one used in Chapter 4, equation (4.29).

The quantum dynamics of the molecule is governed by the time-dependent Schrödinger equation

$$\mathrm{i}\hbar\frac{\partial}{\partial t}\Psi(r,\vartheta,t) = [\hat{\mathrm{H}}_{\mathrm{mol}}(r,\vartheta) + U_{\mathrm{opt}}(r) + \hat{\mathrm{H}}_{\mathrm{int}}(r,\vartheta,t)]\Psi(r,\vartheta,t). \tag{5.6}$$

The wave function and the operators of the equation (5.6) have been transformed from the (r,ϑ) space to the $(r, x = \cos\vartheta)$ space and represented therein on the 256×24-point grid. The radial part was the 256-point equidistant grid with $r_{min} = 0.05\, a_0$, and $r_{max} = 20.0\, a_0$. The angular grid points were the Gauss-Legendre quadrature points $x_k = \cos(\vartheta_k)$, $k = 1, 2, \ldots, 24$, with the respective weights w_k [44, 142]. The time-propagation has been accomplished by a split operator method.

The time step Δt ranged from 0.1 to 0.9 atu. At each time step, the action of the radial part of the kinetic energy operator on the wave function has been evaluated with the fast Fourier transform procedure, and that of the angular part — by making use of the expansion of the wave function in normalized Legendre polynomials, $P_j(x_k),\ j = 0, 1, \ldots, 23$, as described in Ref. [142].

The time-dependent wave function $\Psi(t)$, being projected on the vibrational-rotational eigenstates $|\, v, j \,\rangle$, yields the time-dependent population

$$P_{v,j}(t) = |\langle\, j,\, v \,|\, \Psi(t) \,\rangle|^2. \tag{5.7}$$

The eigenvalue problem with the molecular Hamiltonian (5.3) has been solved for the bound states $|\, v, j \,\rangle$ with $v, j = 0, 1, \ldots, 23$ by the Fourier grid Hamiltonian method [72].

5.2 State-selective excitation and dissociation

As the first target for selective preparation, the moderately high vibrational-rotational state $|\, v = 10, j = 1 \,\rangle$ is chosen. Selective preparation of the target state $|\, 10, 1 \,\rangle$ from the initial one $|\, 0, 0 \,\rangle$ can be achieved by three laser pulses via the intermediate states $|\, 2, 1 \,\rangle$ and $|\, 6, 1 \,\rangle$ according to the excitation pathway

$$|\, 0,\, 0 \,\rangle \rightarrow (1 \text{ photon}) \rightarrow |\, 2,\, 1 \,\rangle \rightarrow (2 \text{ photons}) \rightarrow |\, 6,\, 1 \,\rangle \rightarrow (2 \text{ photons}) \rightarrow |\, 10,\, 1 \,\rangle. \tag{5.8}$$

Each of the three steps is to be selectively controlled by a single laser pulse, which should be optimized to yield the 100% population transfer for the respective transition. The optimization procedure used is similar to that described in Refs. [132,135].

The first step in the excitation pathway (5.8) is the overtone R-transition $|\, 0,\, 0 \,\rangle \rightarrow |\, 2,\, 1 \,\rangle$, while the other two steps are the "one-photon forbidden" Q-type transitions

$$|\, v,\, j \,\rangle \rightarrow (2 \text{ photons}) \rightarrow |\, v + 4,\, j \,\rangle. \tag{5.9}$$

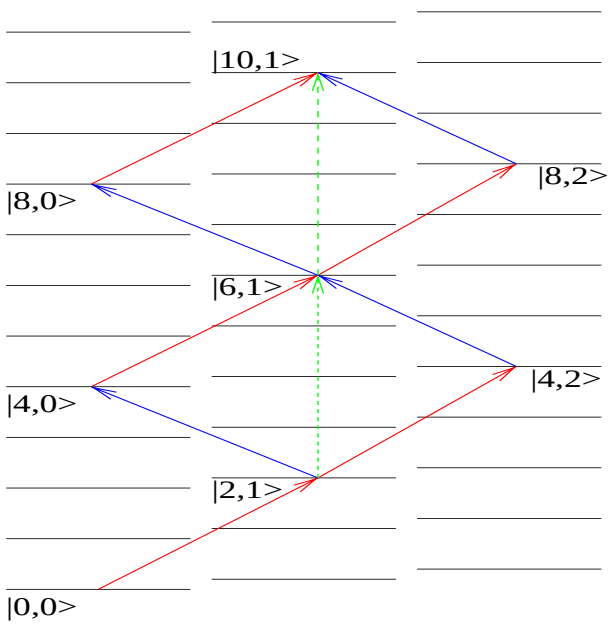

Figure 5.2: Excitation pathway for the preparation of the moderately high $|10, 1\rangle$ state (Equation (5.8))

The idea is that each of these "forbidden" transitions is to be accomplished via two excitation routes, involving two sequential one-photon transitions: the $(R+P)$ route

$$|\, v,\, j\,\rangle \xrightarrow{R} |\, v+2,\, j+1\,\rangle \xrightarrow{P} |\, v+4,\, j\,\rangle, \tag{5.10}$$

and the $(P+R)$ route

$$|\, v,\, j\,\rangle \xrightarrow{P} |\, v+2,\, j-1\,\rangle \xrightarrow{R} |\, v+4,\, j\,\rangle, \tag{5.11}$$

which can interfere constructively providing the complete population transfer (see Figure 5.2). The proposed control scheme is somewhat similar to coherent control as designed by Shapiro and Brumer [143], where two independent excitation routes are controlled by two laser fields. On the contrary, in the case described here, the two routes, (5.10) and (5.11), are to be controlled by a single laser pulse.

The population dynamics controlled by three optimal nonoverlapping 1-ps laser pulses is shown in Figure 5.3a, where the initial, intermediate, and target states are indicated explicitly, and curve "others" gives the overall population of all other bound states. The sequence of three optimal laser pulses is shown in Figure 5.3b. It is

clearly seen that each pulse provides complete population transfer for the respective transition. The final population of the target state at the end of the third pulse is $P_{10,1}(t = 3 \text{ ps}) = 0.9966$. The time-dependent rotational energy of HF is presented in Figure 5.3c. It demonstrates the oscillatory behaviour during each laser pulse and takes, with a very good accuracy, the value of the first rotational quantum of the intermediate and target states at the end of the respective pulse. This serves as an additional demonstration of a very high state selectivity of the process, even at the smallest rotational sublevel spacing corresponding to $j = 1$.

The excitation pathway (5.8) can also be controlled by overlapping laser pulses, which reduce the overall time of the process and provide almost the same population transfer to the target state of the isolated molecule if the overlaps are not too large, for example, not much larger than half of the pulse duration (see also Ref. [135]). Note that overlapping laser pulses may provide much better population transfer than the nonoverlapping pulses if the molecule is coupled to a thermal environment (similarly to overlapping pulses used previously to control dissipative quantum dynamics of rotationless models of OH [136, 137]).

An evident extension of the excitation pathway (8) makes it possible to selectively prepare higher vibrational-rotational states. Now, we assume that the HF molecule is selectively prepared in the moderately high state $|\, v = 10, j = 1 \,\rangle$, as described above, and its laser-induced dissociation from this state is considered.

The dissociation yield is defined by the integrated outgoing flux at $r = r_{opt}$,

$$D(t) = \frac{\hbar}{m_r} \mathrm{Im}\Big(\int_0^t dt' \int_{-1}^{1} dx \Psi^*(r_{opt}, x, t') \, \partial\Psi(r_{opt}, x, t')/\partial r \Big). \qquad (5.12)$$

The approach to the laser-controlled dissociation is described as follows. Starting from selectively prepared state $|\, 10, 1 \,\rangle$, the state $|\, 17, 2 \,\rangle$ is chosen as a higher intermediate state which, being pumped in three-photon resonance, is spaced by less than one photon energy from the continuum. The dissociation is to be controlled by a single 1-ps laser pulse, according to the dissociation pathway

$$|\, 10, 1 \,\rangle \rightarrow (3 \text{ photons}) \rightarrow |\, 17, 2 \,\rangle \rightarrow (1 \text{ photon}) \rightarrow \text{"continuum"}. \qquad (5.13)$$

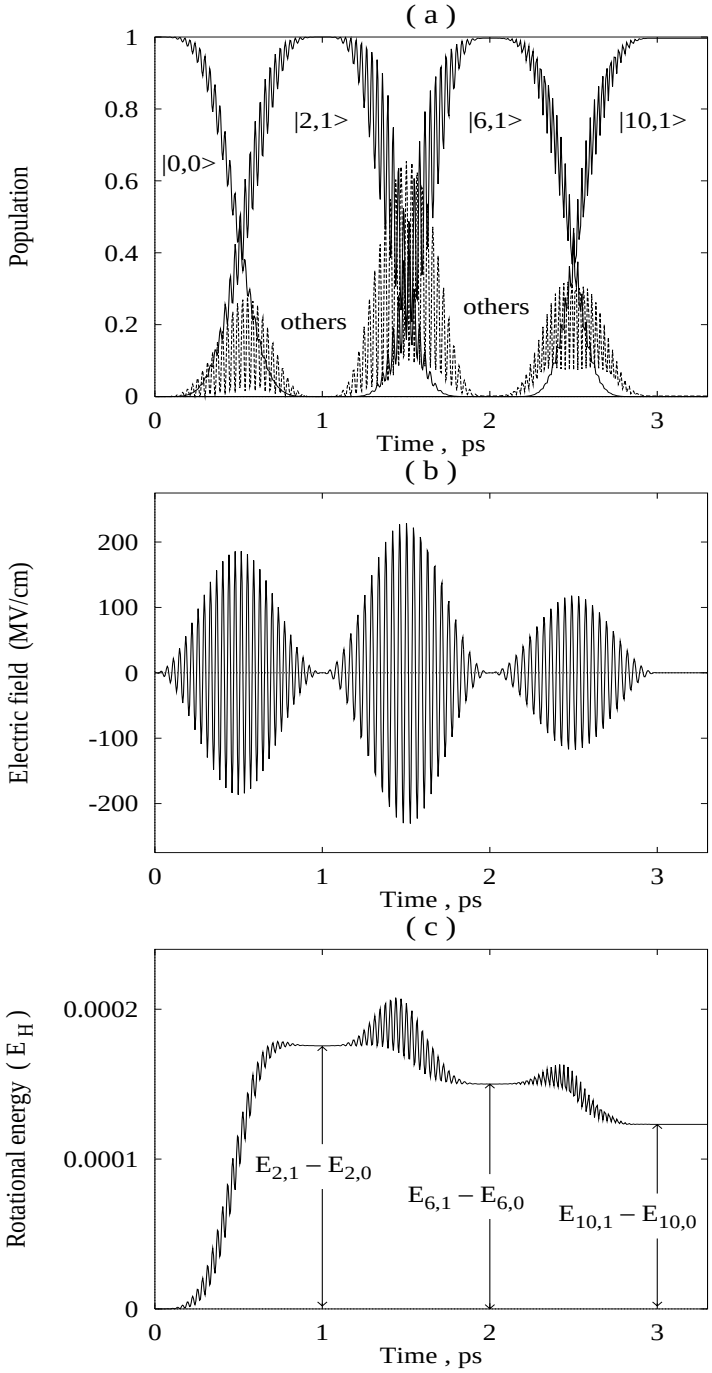

Figure 5.3: Complete population transfer from the initial vibrational-rotational state $|\, v = 0, j = 0 \,\rangle$ to the target state $|\, v = 10, j = 1 \,\rangle$ of HF controlled by three nonoverlapping 1-ps laser pulses. (a) Population dynamics. (b) Optimal laser field: $\mathcal{E}_1^{opt}$ =186.66 MV/cm, ω_1^{opt} =7795.52 cm^{-1}, $\mathcal{E}_2^{opt}$ =233.46 MV/cm, ω_2^{opt} =6710.88 cm^{-1}, $\mathcal{E}_3^{opt}$ =119.81 MV/cm, ω_3^{opt} =5323.80 cm^{-1}. (c) Time-dependent rotational energy of the HF molecule during selective preparation of vibrational-rotational state $|\, v = 10, j = 1 \,\rangle$.

The intermediate state $|\,17,2\,\rangle$ is accessible from the initial one $|\,10,1\,\rangle$ via three interfering excitation routes, involving three sequential one-photon transitions: the $(P+R+R)$ route (see Figure 5.4)

$$|\,10,1\,\rangle \xrightarrow{P} |\,12,0\,\rangle \xrightarrow{R} |\,14,1\,\rangle \xrightarrow{R} |\,17,2\,\rangle, \tag{5.14}$$

the $(R+P+R)$ route

$$|\,10,1\,\rangle \xrightarrow{R} |\,12,2\,\rangle \xrightarrow{P} |\,14,1\,\rangle \xrightarrow{R} |\,17,2\,\rangle, \tag{5.15}$$

and the $(R+R+P)$ route

$$|\,10,1\,\rangle \xrightarrow{R} |\,12,2\,\rangle \xrightarrow{R} |\,14,3\,\rangle \xrightarrow{P} |\,17,2\,\rangle. \tag{5.16}$$

The intermediate state $|\,17,2\,\rangle$ should not be prepared selectively but serves to

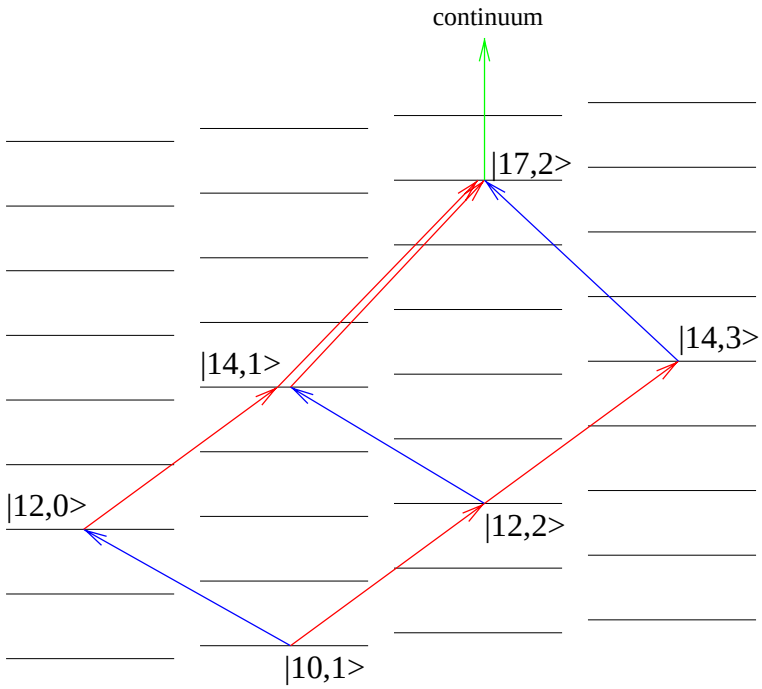

Figure 5.4: Excitation pathway for the dissociation starting from the $|10,1\rangle$ state (Equation (5.13))

enhance the overall dissociation process. The laser carrier frequency is set to the exact three-photon resonance, $\omega_{res} = (E_{17,2} - E_{10,1})/\,3\hbar$, and the dissociation yield

at the end of the pulse as a function of the pulse amplitude is calculated for three pulse durations: $t_p = 0.5$, 1, and 2 ps. The results presented in Figure 5.5a show that the dissociation yield may approach 100%, which is basically a matter of the laser field strength used. Note that while the resonant laser frequency used, $\omega_{res} = 3998.389$ cm^{-1}, is a reasonable initial guess, it is still not optimal for every field strength. An additional optimization of the frequency at a given laser field strength makes it possible to further increase the dissociation yield.

The above considered approach, where use is made of "one-photon forbidden" Q-type transitions (see equations (5.8)-(5.11)), makes it possible to excite a diatomic molecule vibrationally and keep its rotational energy corresponding to a fixed j (for example, $j = 1$ as in Fig. 5.3a). In order to prepare vibrational-rotational states with higher j one can use sequential R-transitions. The example given in Figure 5.5b demonstrates selective preparation of the moderately high target state $|\, v = 11, j = 4 \,\rangle$, followed by the laser-induced dissociation. The preparation stage is accomplished by four overlapping 1-ps laser pulses with the 0.5-ps overlaps of the pulses. The excitation pathway involves four sequential one-photon R-transitions:

$$|\, 0, 0 \,\rangle \xrightarrow{R} |\, 2, 1 \,\rangle \xrightarrow{R} |\, 4, 2 \,\rangle \xrightarrow{R} |\, 7, 3 \,\rangle \xrightarrow{R} |\, 11, 4 \,\rangle. \tag{5.17}$$

The final population of the target state at the end of the fourth laser pulse is $P_{11,4}(t = 2.5 \text{ ps}) = 0.9991$. The dissociation from selectively prepared state $|\, 11, 4 \,\rangle$ is accomplished by two 1-ps laser pulses with the 0.5-ps overlap. The dissociation pathway is chosen as follows:

$$\begin{aligned} |\, 11, 4 \,\rangle \rightarrow (1 \text{ photon}) \rightarrow |\, 16, 5 \,\rangle \rightarrow (4 \text{ photons}) \rightarrow \\ \rightarrow |\, 22, 5 \,\rangle \rightarrow (1 \text{ photon}) \rightarrow \text{"continuum"}. \end{aligned} \tag{5.18}$$

Pathway (18) is based on those used in this work previously. The first step is the overtone R-transition $|\, 11, 4 \,\rangle \rightarrow |\, 16, 5 \,\rangle$. The second step is the "one-photon forbidden" Q-type four-photon transition $|\, 16, 5 \,\rangle \rightarrow |\, 22, 5 \,\rangle$, which is accomplished via six interfering excitation routes from state $|\, 16, 5 \,\rangle$ to state $|\, 22, 5 \,\rangle$, with the latter, being spaced by less than one photon energy from the continuum, serving to enhance the dissociation process. The optimal laser field controlling both the preparation and dissociation stages is shown in Figure 5.5(c) together with the $\sin^2$-shaped envelopes of the overlapping pulses. The final dissociation yield is $D(t = 4 \text{ ps}) = 0.9698$.

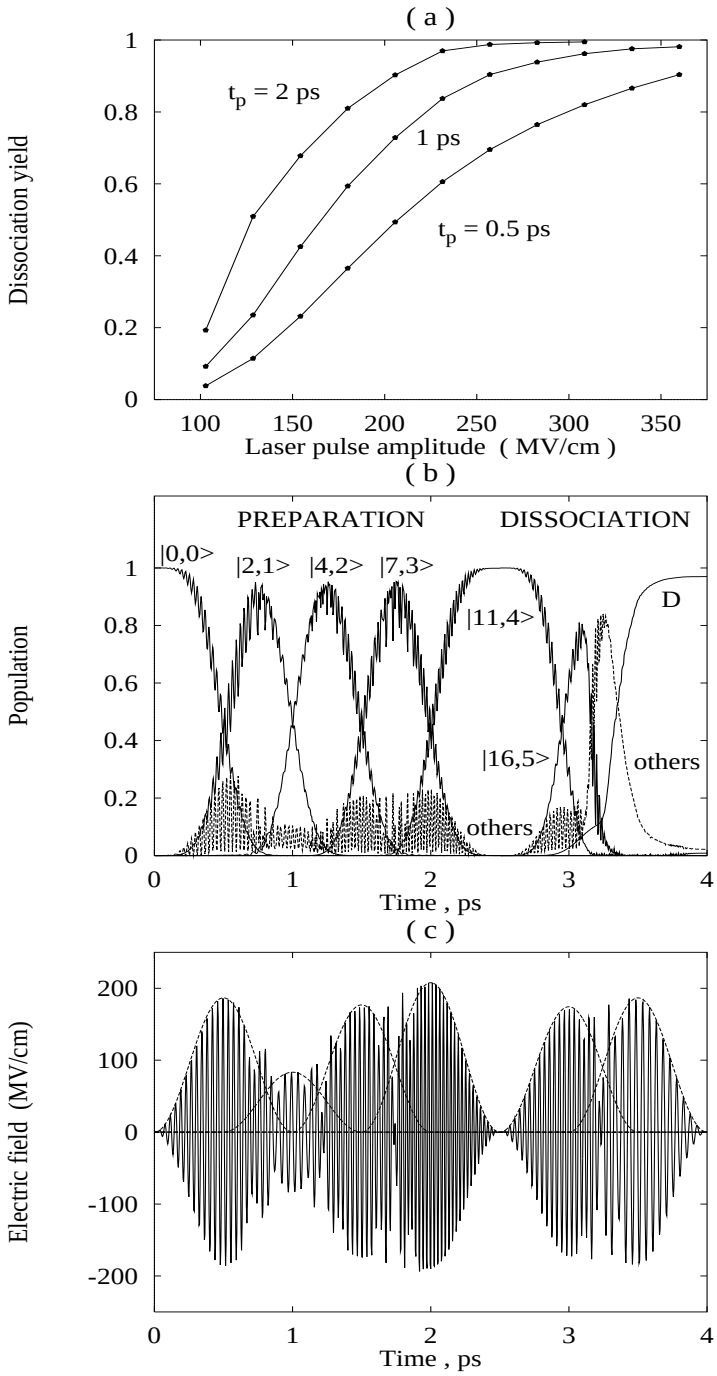

Figure 5.5: Laser-controlled dissociation of HF. (a) Dissociation from state $|\,10,1\,\rangle$ by single laser pulses of the frequency ω_{res}=3998.39 cm^{-1}.. (b) Selective preparation of state $|\,11,4\,\rangle$ controlled by four overlapping 1-ps laser pulses, followed by dissociation controlled by two overlapping 1-ps pulses (the 0.5-ps overlaps are used). (c) Optimal laser field: $\mathcal{E}_1^{opt}$ =186.66 MV/cm, ω_1^{opt} =7795.52 cm^{-1}, $\mathcal{E}_2^{opt}$ =83.30 MV/cm, ω_2^{opt} =7129.41 cm^{-1}, $\mathcal{E}_3^{opt}$ =176.89 MV/cm, ω_3^{opt} =9373.32 cm^{-1}, $\mathcal{E}_4^{opt}$ =207.74 MV/cm, ω_4^{opt} =10029.33 cm^{-1}, $\mathcal{E}_5^{opt}$ =174.32 MV/cm, ω_5^{opt} =8557.75 cm^{-1}, $\mathcal{E}_6^{opt}$ =186.66 MV/cm, ω_6^{opt} =902.98 cm^{-1}.

As already mentioned, the here proposed control schemes are quite flexible with respect to the overlaps of the the laser pulses, when dealing with the isolated molecule. The 0.5 ps overlaps used in the preparation and dissociation stages (5.17) and (5.18) are close to the maximum which still provides almost complete population transfer. Similar dissociation yields (more than 96%) have been obtained with nonoverlapping pulses and with overlapping preparation and dissociation stages.

It should be noted, that the peak intensities of the laser pulses used in the control schemes presented here are quite high. Assuming the typical peak electric field strength used here to be 200 MV/cm, we obtain the intensities of approximately 10^{14} W/cm^2, or 100 TW/cm^2, which, although below the Keldysh limit, is still prohibitively high for most of the current laser systems. Therefore, additional investigations seeking to minimize the strengths of the fields used for the control of vibrational-rotational motion of HF is in order.

5.3 Discussion

The OCT-designed superposition of five subpicosecond IR laser pulses used in Ref. [121] provided the maximal dissociation yield of only 25% for the same model of HF as used in the present work. A brief comparison of our approach with that of Ref. [121] is in order. Rabitz and co-workers [121] have used a superposition of five single-frequency Gaussian pulses with identical fixed amplitudes and widths. The phases of the pulses have been set to zero. With the overall duration of the global laser field being limited to 1.6 ps, the time centers of the five pulses (timings) and their carrier frequencies have been optimized to maximize the dissociation yield. On the contrary, in the approach followed here the timings of the laser pulses are quite flexible for the isolated molecule, while their amplitudes and carrier frequencies are optimized to yield the complete population transfer at every stage of the process. The shorter duration of the global laser field (1.6 ps) used in Ref. [121] seems not to be the main reason of a comparatively small dissociation yield. Several simulations with the 0.5 ps laser pulses for pathways (5.17) and (5.18) have been performed,

thus reducing the time scale to 2 ps, and dissociation yields of about 87% have been calculated. On the other hand, since all optimal laser pulses designed here have different amplitudes, one can assume that the identity of amplitudes of all laser pulses used in Ref. [121] was probably too strong a constraint.